For the potential and detunings shown in Fig. 1, the excitation cross sections are of the order of $10^{-34} II'$ cm^2, with I and I' the power density given in W/cm^2. Thus the effect should be observable with moderate laser power. The experiment must be performed with use of crossed atomic beams or a beam interacting with a gas sample. The beam-gas sample method works only if the active-atom–perturber relative velocity is approximately equal to the beam velocity.

This work was supported by the U. S. Office of Naval Research through Contract No. N00014-77-C-0553. Conversations with Professor E. J. Robinson are acknowledged.

[1]P. R. Berman, in *Advances in Atomic and Molecular Physics*, edited by D. R. Bates and B. Bederson, (Academic, New York, Vol. 13, 1977, pp. 57–112 and references therein.

[2]An extensive list of papers, books, and reviews regarding radiative collision and optical collision for all limits including impact and nonimpact regions can be found in a recent review. See S. I. Yakovlenko, Sov. J. Quantum Electron. 8, 151 (1978).

[3]M. H. Nayfeh, unpublished.

[4]Dressed states are the eigenstates of the active-atom–external-field system. See C. Cohen-Tannoudji, *Cargèse Lecture in Physics* (Gordon and Breach, New York, 1968), Vol. 2, p. 347.

[5]H. Rosenthal and H. M. Foley, Phys. Rev. Lett. 23, 1480 (1969); H. Rosenthal, Phys. Rev. A 4, 1030 (1971).

[6]S. H. Dworetsky and R. Novick, Phys. Rev. Lett. 23, 1484 (1969).

[7]The dressed states and their spacings depend also on the field strengths. In this Letter, the discussion is confined to the weak-field limit.

[8]Similar ideas have been suggested in J. I. Gersten and M. H. Mittleman, J. Phys. B 9, 383 (1976).

[9]For large field intensities, crossings will disappear. See, for example, S. Yeh and P. R. Berman, Phys. Rev. A 19, 1106 (1979).

[10]Equations (7.3.9) and 7.3.10) in M. Abramowitz and I. A. Stegun, *Handbook of Mathematical Functions* (Dover, New York, 1972), p. 301.

Temporally Recurrent Spatial Ordering of Atomic Population in Gases: Grating Echoes

T. W. Mossberg, R. Kachru, E. Whittaker, and S. R. Hartmann
Columbia Radiation Laboratory, Department of Physics, Columbia University, New York, New York 10027
(Received 23 July 1979)

We predict and observe the periodic reformation of spatial gratings in Na vapor commencing $\tau/2$ after the application of the second of two resonant ($\lambda = 5896$ Å) standing-wave excitation pulses which are themselves separated by τ. These gratings have spatial periodicity $\lambda/2$, and backscatter our laser. One set of alternate echoes relaxes because of velocity-changing collisions; phase-changing collisions play no role. The other set is amplitude modulated with laser detuning Δ as $\cos\Delta\tau$.

Since the observation of the photon echo in ruby[1] in 1964 and its extension[2] to a gaseous medium in 1968, a variety of optical echo phenomena have been discovered in gases. These effects include the trilevel echo,[3] the two-photon echo,[4] the optical stimulated echo,[5,6] and the two-pulse standing-wave (SW) photon echo.[7,8] These echoes are similar inasmuch as they are all formed from *a delayed reordering of atomic superposition states*. In this Letter we report the observation of an effect which belongs to an *entirely new class of reordering phenomena* and is characterized by spatial reordering of atomic *populations*. The spatially reordered populations constitute "gratings" and can be detected by scattering a probe beam from them.[9] We term these delayed gratings "grating echoes."

We find that the excitation of atoms in a gaseous sample by two resonant collinear SW fields, separated in time by τ, gives rise to grating echoes which have spatial periodicity $\lambda/2\beta$, where $\beta = 1, 2, \ldots$ and which appear repetitively at the times $n\tau/2\beta$ after the second SW field. Here λ is the wavelength associated with the transition excited by the SW fields, and $n = 1, 2, \ldots$ for each β. For $\beta = 1$ the grating echoes have a spatial periodicity of $\lambda/2$ and occur every $\tau/2$ after the second SW excitation pulse. Working on the $3S_{1/2}$-$3P_{1/2}$ transition of Na we have observed the first two $\beta = 1$ grating echoes. In Fig. 1 we present a photograph showing the scatter from the first ($n = 1$) grating echo together with the two SW excitation pulses. Given that two SW excitation fields have been shown to produce photon echoes which appear every τ after the second SW field, it is not surprising that grating echoes reappear at equally

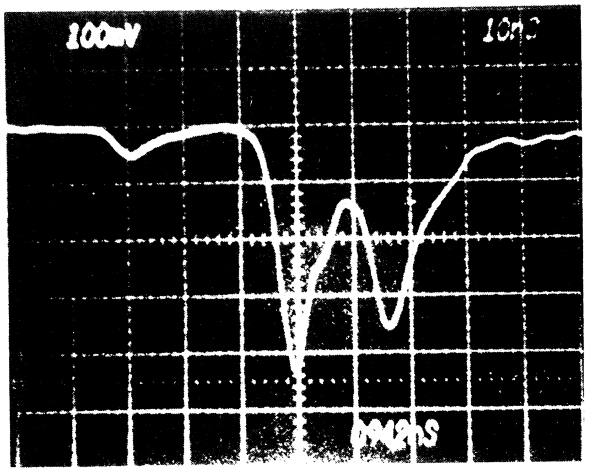

FIG. 1. Oscilloscope trace showing (from left to right) instrumentally scattered light from the first and second standing-wave excitation pulses and the probe light backscattered from the $\beta = n = 1$ grating echo. This grating echo has spatial periodicity $\lambda/2$ and occurs delayed from the second SW pulse by $\tau/2$. (Horizontal scale: 10 nsec/div; vertical scale: 100 mV/div.)

spaced intervals. The $\tau/2\beta$ interval, however, is unexpected.

Grating echoes have a number of novel and important properties. In contrast to all other optical echoes, certain grating echoes are unaffected by the phase-changing aspect of collisions throughout their *entire evolution*. Consequently, they are degraded only by collisionally induced changes of state or velocity. Like the stimulated photon echo,[6] grating echoes can be used to study collisional effects pertaining to *single* isolated energy states. Unlike the common two-pulse photon echo,[1,2] but like SW photon echoes,[7,8] grating echoes are produced only when the excitation fields have spectral components overlapping a natural atomic frequency ω_0 (i.e., Doppler-free excitation). Furthermore both SW photon echoes and certain grating echoes exhibit oscillations in magnitude as the excitation laser central frequency, ω, is varied about ω_0. This oscillation, which arises from an effect similar to that responsible for Ramsey fringes,[10] may allow resolution of spectroscopic detail normally obscured by the spectral width of the excitation pulses.

Assume that the first (second) SW pulse occurs at the time t_1 (t_2), is linearly polarized along $\hat{x}$, has the form

$$\hat{x}\mathcal{E}_1 \cos(\omega t)\cos(kz)[\hat{x}\mathcal{E}_2 \cos(\omega t)\cos(kz+\varphi)],$$

and is nearly resonant with the $|g\rangle$-$|e\rangle$ transition (having frequency ω_0) of the atoms in a Doppler-broadened gaseous sample. Here $\vec{k} \equiv (\omega/c)\hat{z}$. The levels $|g\rangle$ and $|e\rangle$ refer to the atom's ground and an initially unpopulated excited state, respectively. The temporal duration of each excitation pulse, t_p, is assumed to be sufficiently short that atomic motion during the excitation pulses can be neglected. The area of the first [second] SW pulse varies with position as $\theta_1(z) = \theta_1{}^0 \cos(kz)$ [$\theta_2(z) = \theta_2{}^0 \cos(kz+\varphi)$], where $\theta_l{}^0 = p\mathcal{E}_l t_p/\hbar$ ($l = 1, 2$), $p = |\langle g|\vec{p}\cdot\hat{x}|e\rangle|$, and $\vec{p}$ is the electric dipole operator. After the two SW pulses the probability that an atom, which was at position z_l during the lth SW pulse, will be in state $|g\rangle$ is given by

$$\rho_{gg} = \tfrac{1}{2}[1 + \cos\theta_1(z_1)\cos\theta_2(z_2) - \sin\theta_1(z_1)\sin\theta_2(z_2)\cos\Delta\tau], \tag{1}$$

where $\Delta \equiv \omega - \omega_0$. Expanding Eq. (1) in terms of Bessel functions we obtain

$$2\rho_{gg} = 1 + \tfrac{1}{4}\sum_{m,n=-\infty}^{\infty} (i)^{m+n} \exp[ik(mz_1 + nz_2)] \exp(in\varphi) J_m(\theta_1{}^0) J_n(\theta_2{}^0) \cdot [1 + (-1)^{m+n}]\{[1 + (-1)^n] + [1 - (-1)^n]\cos\Delta\tau\}, \tag{2}$$

where J_l is a Bessel's function of order l. The fraction of atoms in level $|g\rangle$ at a particular position z at some time $t > t_2$, which we denote $\eta_g(z,t)$, is determined by averaging Eq. (2) over all atoms at z at time t. Assuming that v, the z component of velocity (z velocity), is constant, we can write $z_l = z - v(t - t_l)$. Then ρ_{gg} can be expressed as

$$2\rho_{gg} = 1 + \sum_{n=0}^{\infty} (-1)^n \cos\{kvnt_2 - n\varphi\} J_n(\theta_1{}^0) J_n(\theta_2{}^0)\{[1 + (-1)^n] + [1 - (-1)^n\cos\Delta\tau\} + \sum_{\beta=1}^{\infty} (-1)^\beta \sum_{n=-\infty}^{\infty} (-1)^n \cos\{2\beta kz - 2\beta kv[t - (1 + n/2\beta)t_2] + (n + 2\beta)\varphi\} \times J_n(\theta_1{}^0) J_{n+2\beta}(\theta_2{}^0)\{[1 + (-1)^n] + [1 - (-1)^n\cos\Delta\tau\}. \tag{3}$$

In Eq. (3) and hereafter we set $t_1 = 0$. $\eta_g(z,t)$ is now obtained by averaging ρ_{gg} over the Maxwellian z-velocity distribution. From Eq. (3) it can be seen that the dependence of $\eta_g(z,t)$ on z will be washed out

unless

$$t = t_e = (1 + n/2\beta)t_2 . \tag{4}$$

The spatial periodicity of $\eta_g(z, t_e)$ is $\pi/\beta k = \lambda/2\beta$, where β corresponds to the term in Eq. (3) for which the coefficient of v vanishes. The amplitude of the spatial modulation of $\eta_g(z, t_e)$ is proportional to $J_n(\theta_1{}^0)J_{n+2\beta}(\theta_2{}^0)$, which can be comparable to unity for appropriate $\theta_1{}^0$ and $\theta_2{}^0$ when β and n are small. Thus as stated above, spatial gratings of periodicity $\lambda/2\beta$ appear every $\tau/2\beta$ after the second SW pulse.

An interesting dichotomy appears in the grating echoes which arise from terms of Eq. (3) having odd and even values of n. The odd n terms appear multiplied by the factor $\cos\Delta\tau$, indicating that their magnitude oscillates as the central laser frequency is tuned about ω_0. These oscillations occur *within* the spectral width of the excitation pulses, introducing an effective spectral narrowing which can be used profitably in spectroscopy. The even-n terms on the other hand exhibit no oscillatory dependence on $\Delta\tau$.

Even-n terms are important since superposition states play no role in the evolution of the corresponding grating echoes, thereby allowing unambiguous studies of velocity-changing collisions (VCC). Collisional phase changes can only influence the evolution of grating echoes during the interval between t_1 and t_2. If during that interval an atom experiences a collisional phase change of θ_p, its density matrix element ρ_{gg} is modified by replacing $\cos\Delta\tau$ with $\cos(\Delta\tau + \theta_p)$. But only odd n terms are modified by this replacement. It follows then that even n terms are insensitive to phase-changing collisions. Considering only the effects of VCC, the electric field, $\mathcal{E}_S$, of the signal scattered by the grating echo which reforms at $(1+N)\tau$, where $N = 1, 2, \ldots$ (we specialize here to $\beta = 1$ and n even) varies as

$$\mathcal{E}_S \sim \langle \cos\{2k[\int_0^{(1+N)\tau} v(t)dt - (1+N)\int_0^{\tau} v(t)dt]\}\rangle . \tag{5}$$

This is a generalization of Eq. (3). Here $v(t)$ is the instantaneous atomic z velocity, and the angular brackets indicate an average over all possible collisions. With k replacing $2k$, Eq. (5) becomes proportional to the amplitude of the Nth two-pulse SW echo.[8] From the analysis of Le Gouët and Berman[8] it then follows that the scattered radiation field relaxes as

$$\mathcal{E}_S \propto \exp\{-(1+N)\Gamma\tau[1 - \tau^{-1}\int_0^{\tau} dt \int_{-\infty}^{\infty} d(\delta)\exp\{2ikN\delta t\}f(\delta)]\}, \tag{6}$$

where Γ is the total VCC rate, δ is the z-velocity change introduced by a single VCC, and $f(\delta)$ is a weak-collision scattering kernel. Analysis of grating-echo relaxation, without corrections for phase-changing collisional relaxation, allows the determination of Γ and $f(\delta)$.

If a traveling-wave probe beam of wave vector k_p is incident on a grating of spatial periodicity π/k_g as shown in Fig. 2(a), a scattered wave will be emitted as shown if

$$\cos\psi = lk_g/k_p , \tag{7}$$

where $l = \pm 1, \pm 2, \ldots$. Setting $l = 1$ and $\psi = 0$, we see that the condition $k_p \geq k_g$ must be satisfied for scattering to occur. It follows that if (as assumed above) the traveling-wave components of the SW field exactly counterpropagate along $\hat{z}$, which implies $k_g = \beta k$, and if $k_p = k$ only gratings corresponding to $\beta = 1$ can be observed. However, if the probe is resonant with a higher-frequency transition, higher-β gratings are also detectable. When $k = k_p$ the gratings formed by the excited-state population also participate in the scattering. Since it can be shown that corresponding ground- and excited-state gratings are spatially displaced along $\hat{z}$ by one-half the grating period from one another, the scattering in the backward direction

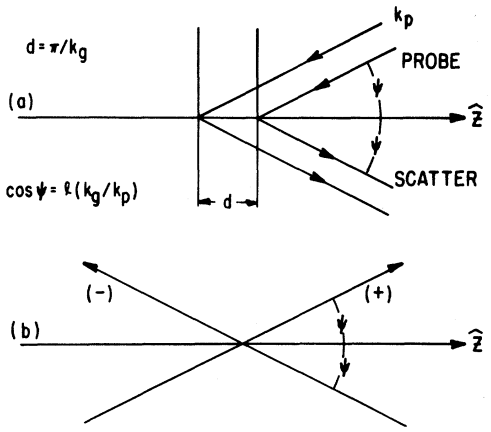

FIG. 2. (a) Scattering of a probe beam from scattering planes periodically spaced along $\hat{z}$. (b) Relative propagation directions of the traveling-wave components of the two SW excitation fields. The scattering planes formed during the grating echoes resulting from these pulses are normal to $\hat{z}$ [as shown in (a)].

[Fig. 2(a)] from both gratings adds constructively. In forward-directed scattering processes the signals from the two populations add destructively. Scattering from either ground- or excited-state echo gratings separately is expected whenever the probe excites a transition involving only one of the states $|g\rangle$ or $|e\rangle$.

To demonstrate the existence of grating echoes we have performed an experiment on the 589.6-nm $3S_{1/2}$-$3P_{1/2}$ transition of Na. Excitation pulses were obtained by amplifying the 10-mW output of a single-longitudinal-mode cw dye laser by injecting it into a Hänsch-type N_2-laser-pumped dye laser (with end mirror removed). The kilowatt-peak-power 3.5-nsec full width at half maximum (FWHM) pulse was suitably optically divided and delayed to provide two temporally separated SW excitation fields and a traveling-wave probe. The oppositely directed components of the SW fields (+ and −) were directed through the heat-pipe-type Na cell (maintained at 450 K) at an angle $\psi \cong 8$–10 mrad on opposite sides of the Na cell axis ($\hat{z}$) in the y-z plane [see Fig. 2(b)]. The angle ψ, introduced to facilitate the detection of the grating echoes, modifies their properties inasmuch as the spatial periodicities change from $k_g = \beta k$ to $k_g = \beta k \cos\psi$ and odd-n grating echoes are reduced in amplitude by $\langle \cos[(v_y k\tau/2)\sin\psi]\rangle$. Here the angular brackets indicate an average over v_y, the y component of atomic velocity. Since $k = k_p$ in our experiments, Eq. (7) is satisfied for $\beta = 1$ if the probe is also directed at the angle ψ with respect to $\hat{z}$ [Fig. 2(a)]. The grating-echo-induced scattering of the probe then occurs in a direction isolated from the excitation fields. To prevent instrumental scatter of the SW excitation fields from reaching the photomultiplier-tube detector an electro-optic shutter, gated to open after the second SW field, was placed in the path of the grating echo. Filters were employed to reduce the peak powers of the traveling-wave components of the SW fields and the probe (all collimated with $\cong 2$ mm diameters) to roughly 0.1–1 W.

We have observed the $\beta = 1$ grating echoes which occur at $t_e(n=1) = t_2 + \tau/2$ and $t_e(n=2) = t_2 + \tau$. The $n = 1$ ($n = 2$) grating echo was observed with $\tau = 21$ and 28 nsec ($\tau = 21$ nsec). To ensure that the gratings were indeed reforming at the expected times, the probe time t_3 was varied about t_e. Both the $n = 1$ and $n = 2$ grating-echo signals were found to be localized in time to a 5–6-nsec region, centered at $t_e - t_3 \cong 2$ nsec. The fact that the gratings obtained their maximum amplitude slightly before the expected echo time may arise from subtle effects of excitation pulse shape and duration which we have neglected in our analysis. The grating-echo scattering efficiency ($I_{\text{scatt probe}}/I_{\text{probe}}$) was $\cong 2\times 10^{-6}$. This low efficiency results in part from relaxation of the 16-nsec-lifetime $3P_{1/2}$ state.

As expected grating echoes were only observed when ω was resonant with the transitions of $v = 0$ atoms between the $3S$-state hyperfine components (split by 1772 MHz) and the $3P_{1/2}$ state. The large spectral width ($\gtrsim 200$ MHz FWHM) of our short transform-limited excitation pulses precluded the resolution of the $3P_{1/2}$ hyperfine structure (189 MHz). We were unable to see the $\cos\Delta\tau$ oscillation of the $\tau/2$ grating-echo signal versus Δ (with a period of 24 MHz for $\tau \cong 21$ nsec). This presumably results because of our large ($\cong 30$ MHz) cw-laser linewidth.

In conclusion, we have shown that various harmonics of the spatial ordering of atomic density introduced in a gaseous sample by a SW excitation pulse can be induced to reappear at later times by a second SW excitation pulse. In particular spatial gratings of periodicity $\lambda/2\beta$ occur every $\tau/2\beta$ after the second SW field. The "grating echoes" can be detected by scattering a resonant (or possibly nonresonant) probe pulse from them. Certain grating echoes are completely unaffected by the phase-changing aspect of collisions. Others, through a Ramsey-fringe-type effect, may prove useful in high-resolution spectroscopy.

This work was supported by the Joint Services Electronics Program under Contract No. DAAG 29-79-C-0079 and by the U. S. Office of Naval Research under Contract No. N00014-78-C-517.

[1]N. A. Kurnit, I. D. Abella, and S. R. Hartmann, Phys. Rev. Lett. 13, 567 (1964).

[2]C. K. N. Patel and R. E. Slusher, Phys. Rev. Lett. 20, 1087 (1968).

[3]T. Mossberg, A. Flusberg, R. Kachru, and S. R. Hartmann, Phys. Rev. Lett. 39, 1523 (1977).

[4]A. Flusberg, T. Mossberg, R. Kachru, and S. R. Hartmann, Phys. Rev. Lett. 41, 305 (1978).

[5]M. Fujita, H. Nakatsuka, H. Nakanishi, and M. Matsuoka, Phys. Rev. Lett. 42, 974 (1979).

[6]T. Mossberg, A. Flusberg, R. Kachru, and S. R. Hartmann, Phys. Rev. Lett. 42, 1665 (1979).

[7]V. P. Chebotayev, N. M. Dyuba, M. I. Skvortsov, and L. S. Vasilenko, Appl. Phys. 15, 319 (1978).

[8]J.-L. Le Gouët and P. R. Berman, Phys. Rev. A (to be published).

[9]The formation of transient gratings by optical interference and their detection by light scattering is well known. Previously, however, the gratings have been found to arise during excitation and to exhibit monotonic decay thereafter. See D. W. Phillion, D. J. Kuizenga, and A. E. Siegman, Appl. Phys. Lett. 27, 85 (1975), and references therein.

[10]J. C. Bergquist, S. A. Lee, and J. L. Hall, Phys. Rev. Lett. 38, 159 (1977); V. P. Chebotayev, Appl. Phys. 15, 219 (1978).

Radial Transport in ELMO Bumpy Torus with Constant Edge Neutral Flux

E. F. Jaeger and C. L. Hedrick
Oak Ridge National Laboratory, Oak Ridge, Tennessee 37830

and

W. B. Ard
McDonnell-Douglas Research Laboratories, St. Louis, Missouri 63166

(Received 18 June 1979)

One-dimensional radial transport equations for the ELMO bumpy torus are solved numerically assuming a constant flux of cold neutrals at the plasma edge. With this boundary condition, thermal stability of numerical solutions is achieved, for the first time, in the collisionless electron regime using a fully classical transport model. Results show a parametric dependence on edge neutral pressure in the collisionless regime which is similar to that observed in experiments.

Recently, one-dimensional (1D) radial transport calculations[1,2] for the ELMO bumpy torus (EBT)[3] have assumed a variable flux of cold neutrals at the plasma edge determined by instantaneous reflux of toroidal plasma particles from the wall. This leads to thermally unstable numerical solutions[2] in the collisionless electron regime where, by contrast, experiments operate stably.[3] In this paper we apply an alternative boundary condition that assumes a constant flux of cold neutrals at the plasma edge independent of toroidal plasma parameters. Such a boundary condition is appropriate if reflux from the wall occurs on a time scale that is slow compared with the energy containment time. Experiments[3] indicate that a time on the order of tens of minutes is required for the plasma to reach equilibrium with the wall. Once equilibrium is reached, pumping is balanced by a slight gas feed of $\sim 3\times10^{-2}$ Torr liter/s. This feed rate is small compared to the flux of neutrals required to sustain the plasma that is ~ 1 Torr liter/s in the present calculations. The source of these neutrals is assumed to be wall reflux.[3]

The 1D radial transport equations for EBT incorporating a self-consistent radial electric field have been discussed elsewhere.[1,2,4] The present calculations are based on a numerical solution to these equations, assuming approximate neoclassical transport coefficients that include lowest-order effects of velocity-space regions where poloidal drift frequencies are small.[2,5] For particles that experience cancellation of electric and magnetic drifts in the bulk of the velocity-space distribution (ions in EBT), the flux is dominated by slowly orbiting particles on noncircular drift orbits. In the moderate collisionality (plateau) regime, this gives transport coefficients independent of collision frequency.[2,5] Specifically, the plateau result of Eq. (14) (Ref. 2) is used for ions. For particles that do not experience such a bulk cancellation of drifts (electrons in EBT), the flux is dominated by particles with large poloidal drift frequencies and nearly circular orbits. For convenience, the large-electric-field result of Kovrizknykh[6] is used for electrons.

Numerical transport solutions in Ref. 2 assume the flux of cold neutrals at the plasma edge to be determined by the toroidal plasma through instantaneous reflux of plasma particles at the wall. In this approximation the total number of plasma particles remains constant in time. In the collisionless regime, energy containment time increases with electron temperature, and for a constant total number of particles, there is a net positive feedback in the numerical calculations in Ref. 2, causing lifetime and temperature to become arbitrarily large. Steady-state solutions exist only if the temperature dependence of the energy lifetime is modified artificially at low collisionalities.[2]

In contrast, calculations in this Letter assume

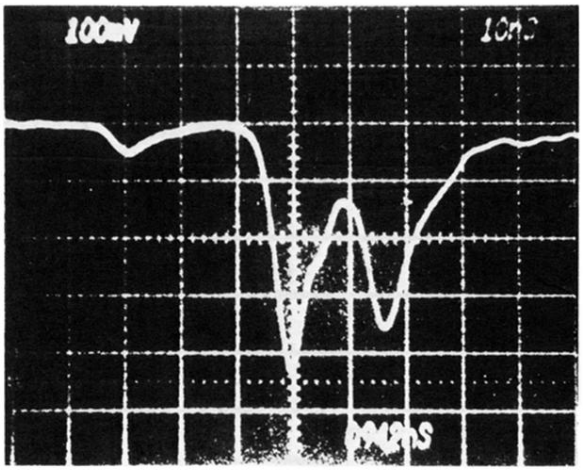

FIG. 1. Oscilloscope trace showing (from left to right) instrumentally scattered light from the first and second standing-wave excitation pulses and the probe light backscattered from the $\beta = n = 1$ grating echo. This grating echo has spatial periodicity $\lambda/2$ and occurs delayed from the second SW pulse by $\tau/2$. (Horizontal scale: 10 nsec/div; vertical scale: 100 mV/div.)